Available online at www.sciencedirect.com

ScienceDirect

Physics Procedia 55 (2014) 396 – 402

Physics Procedia

Eighth International Conference on Material Sciences, CSM8-ISM5

Control of spatial organization of gold nanoparticles using Cylindrical Nanopores of Block Copolymers Films

M. Rajab[a,b], K. Mougin[a], M. Derivaz[a], D. Dentel[a] L. Josien[a], L. Vidal[a], V. Luchnikov[a], T. Hamieh[b,c*], K. Hariri[b], J. Toufaily[b], H. Haidara[a]

[a] Institut de Science des Matériaux de Mulhouse (IS2M), CNRS, UPR 9096, 15 Rue Jean Starcky, B.P. 2488 - 68057, Mulhouse Cedex, France

[b] *Laboratory of Materials, Catalysis, Environment and Analytical Methods, Faculty of Sciences I, PRASE- EDST, Lebanese University, Campus Rafic Hariri, Beirut, Lebanon*

[c] *Faculty of Agricultural Engineering and Veterinary Medicine, Lebanese University Dekwaneh, Beirut, Lebanon*

Abstract

In this paper, a sequential process of elaboration of hybrid nanostructured composite films has been proposed. The combination of phase separation in poly(styrene-block-4vinylpyridine) (PS-P4VP) block copolymer leading to the formation of nanopores, and gold nanocolloids synthesis confined in the nanoholes has allowed the facile fabrication of hexagonally arranged gold nanoparticles (NPs) onto silicon wafer. In particular, the nucleation and growth of gold nanoparticles took place within the nanopores, where they are confined in both size and shape the formed Au NPs. The resulting hybrid nanoscomposite has been characterized by Atomic Force Microscopy (AFM) and X-Ray Spectroscopy (XPS). This facile and simple process represents an opened pathway to several technologically important materials fabrication such as hierarchical and ordered crystal architectures. Indeed, the approach based on solvent phase, which is particularly attractive due to its low energy requirement, and the safety and environmentally gentle processing conditions.

Peer-review under responsibility of the Organizing Committee of CSM8-ISM5

Keywords: block copolymer, self-assembly, soft synthesis route, colloidal nanoparticles, hexagonal and square ordering

1. Introduction

Nanostructured films and coatings with controlled surface functionnality, porosity, crystalline orientation, grain sizes, and crystal morphologies are desirable for many applications, including microelectronic devices, chemical and biological sensing, energy conversion and storage (photovoltaic cells, batteries and capacitors, and hydrogen-storage devices), light-emitting displays, catalysis, drug delivery, separation, and optical storage [1-2].

* Corresponding author. Tel.: 00-961-3-968-850; fax: 00-961-1-510-870.
E-mail address: tayssir.hamieh@ul.edu.lb

Peer-review under responsibility of the Organizing Committee of CSM8-ISM5
doi:10.1016/j.phpro.2014.07.057

However, control of the structure and properties of materials at the nanoscale still represents a key challenge associated with the development of nanostructured materials. One route to reach this goal is the "bottom- up" approach. Among all the possibilities in this domain, self-assembly process represents a crucial strategy to build the blocks of future advanced nanoscale materials[3]. Alternatively, "top-down" lithographic approaches offer arbitrary geometrical designs and superior nanometer-level precision, accuracy, and registration. However lithography techniques are very expensive and do not permit to obtain highly dense nanoscale patterns [4]. At the opposite, self-organizing materials provide simple and cost effective processes to make large-area periodic nanostructures [5- 6].In particular, self-assembly processes of block copolymers offer interesting possibilities to create patterns on nanometer length scales. Nanoporous copolymer films can be realized by selective removal of one of the blocks via degradation upon UV radiation, [7] plasma etching, [8] or extraction of alow molecular mass additive that forms supramolecular assemblies. [9]. The polymeric constituents, substrate surface properties, and experimental conditions all offer parameters that allow the control and optimization of pattern formation for specific applications and to produce well-registered nanostructures. [10]

Then, an alternative approach is to build-up nanosized structures and devices by using nanoscale building blocks to initiate growth directly at desired positions and with designed dimensions and properties. Recently, significant progress in the synthesis of complex nanostructures through sequential nucleation and growth processes has been done[11]. The use of multistage, seeded-growth methods to synthesize a wide range of nanostructures, such as oriented nanowires, nanotubes, and nanoneedles and multilayer heterostructures[12] has been initiated. However, these methods typically require high temperatures (500–1100 °C) and vacuum conditions, which limit the choice of substrate and the economic viability of high-volume production[13]. These limitations have stimulated research on solution-phase synthesis, also referred to as *soft solution route* or *chemical bath deposition*, which offers at the opposite, the potential for low-cost, industrial-scale manufacturing. Indeed, low-temperature (typically < 100 °C), aqueous-phase approaches are particularly attractive because of their low energy requirements, and the safety, and environmentally gentle processing conditions[14].

Finally, the combination of block copolymer phase separation and solution-phase synthesis of colloids represents a simple method to fabricate hybrid materials. These materials represent an important class of functional hard/soft hybrid composites. In particular, this method is well adapted to the synthesis and self-assembly of inorganic nanoparticles (NPs) within the structures of ordered A-b-B dibock copolymers (BCPs) [15]. The ability to systematically modify the shapes of such inorganic nanocrystals is an important goal in materials chemistry today[16]. Hence, in aqueous-phase synthesis, oriented nanocrystalline films are deposited on a substrate in aqueous media by heterogeneous nucleation and subsequent growth. For instance, the growth of ZnO NWs onto various substrates using thermal decomposition of methylamine and zinc nitrate in aqueous solution was reported by several groups [17]. A multistep, seeded-growth technique developed by the Liu and co-workers [18] allows control of the sequential nucleation and growth, leading to complex nanostructures composed of hierarchical nanorods.

Here, we report a method of fabrication of patterned arrays of gold nanoparticles. The hexagonal arrangement of the gold nanocolloids has been induced by a block copolymer template. To prepare effectively the golden array on a substrate, a cleaned surface of silicon wafer was used to precoat the thin film of block copolymer PS-P4VP mixed with HABA. The mask layer of the block copolymer with patterned nanopores was then realized on the substrate using solvent annealing to form of ordered domains, which either exhibit hexagonnal or square lattice packing. These nanodomains are then removed by HABA treatment leading to the formation of nanoholes. The polymer template was finally immersed in a $HAuCl_4$ solution. The $HAuCl_4$ salt that preferentially attach to the P4VP blocks, has been reduced by hydrazine, monohydrate solution. The synthesis of gold colloidal nanoparticles within polymer nanoholes, referred to as "nanoreactor concept", because the chemical reaction from the precursor to the nanoparticle takes place within the opened PVP columns, which themselves confined the size of the formed nanoparticles. After the removal of the polymer phase, the nanostructured surface, which has been characterized by Atomic Force Microscopy in Tapping mode and XPS mainly presents a hexagonal arrangement of Au nanoparticles, perfect negative replication of predefined features. This approach provides a method for the design and synthesis of controlled 3D architectures in nanostructured films.

2. Experimental

2.1. Materials

The PS-b-P4VP diblock copolymers (BCP) of number average molecular weigth, M_n = 45 600 g.mol^{-1} were purchased from Polymer Source, inc. The molecular weights of PS and P4VP blocks were M_n= 40 000 and 5600 g.mol^{-1} respectively. The films are prepared by codissolving polystyrene-block-poly(4-vinylpyridine) (PS-b-P4VP) and 2-(4-hydroxyphenylazo)benzoic acid (HABA) that is associated with the P4VP block by hydrogen bonds. HABA and chloroform were purchased from Sigma Aldrich. All chemicals were used as received.

1. Silicon surface

Silicon wafer were cut and cleaned in ultrasonic bath of cyclohexane for 5 min. They were heated at 60 °C in cleaning solution of NH_4OH, H_2O, and Millipore water, in ratio 3 : 3 : 4 for 90 min (until all peroxide evaporates). Finally, they were thoroughly rinsed with Millipore water and dried under a nitrogen flow.

2. . Block copolymer:

Thin films of poly(styrene-b-4-vinyl pyridine) diblock copolymer mixed with HABA into chloroform. The BCP mixture was deposited by dip-coating onto cleaned silicon surface from the 1.5 wt.-% solution in chloroform and annealed in vapor of 1,4-dioxane for 4 days. P4VP & HABA complexes form cylinders, which are aligned along the normal direction to the film and embedded into the PS matrix as displayed in Figure 1. HABA was removed by dipping the BCP polymer in a methanol bath for 5min and dried under a nitrogen flow. At the surface, this asymmetric diblock copolymer self-assembles into hexagonally packed arrays of cylindrical microdomains with diameters of 20 nm with a mean separation of ~15 nm. Thanks to UV degradation of aromatic hydrocarbons to aliphatic radicals, porous PS-*b*-P4VP nanotemplates was cross-linked. The required irradiation dose of about 2 J/cm² is achieved upon 40 min of irradiation at 254 nm with a UV lamp, when the films are placed 15 cm from the lamp tube [19].

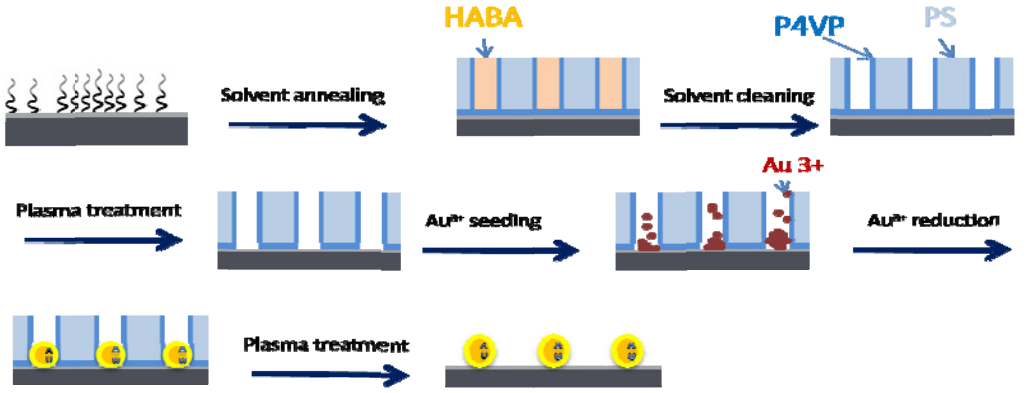

Figure 1: Scheme depicting the sequential procedure of assembling the PS-P4VP onto cleaned silicon wafer .

Golden salt was added to the copolymer by immersing the BCP template film in an 1% aqueous solution for several hours. After this imbibition step, the tetrachloroauric acid salt was reduced by the addition of solution of hydrazine or $NaBH_4$. The sample was then dried. Then, the polymer was removed using an oxygen plasma (90 W, 300 mTorr, 10 min) treatment. Such a treatment also causes the reduction of Au^{3+} to Au^0 (by oxidation of the complexe components) and allows the gold to nucleate to a nanometer-sized

crystalline Au particle[19-22]. Complete removal of the polymer was assssesd using the carbon signal by an X-ray photoelectron spectroscopy (XPS).

2.3. Characterization

Atomic Force Microscopy (AFM)

The atomic force microscopy images of the BCP and hybrid films were performed using the Bruker scanning probe microscope –multimode equipped with a nanoscope V contrller in Tapping mode. The AFM scans were interpreted using the Nanoscope Analysis software.

Ellispsometry

Film thicknesses were determined by null-ellipsometry (Multiskop, Optrel, Berlin, Germany[23]. All measurements were done under ambient conditions at 70° angle of incidence using a He-Ne laser (λ = 632.8 nm). Film calculations were performed using the Elli software (Optrel). The refractive index, n, and absorption coefficient, k, of the substrate were determined from bare silicon surfaces using a 2-phase model (air/substrate). The thickness of the copolymer film was then calculated using a 3-phase model (air/film/substrate) assuming that film optical constants were n = 1.46 and k = 0.

3. Results and Discussion

This multistep synthesis of complex nanostructured films starts with substrate surface preparation for heterogeneous nucleation of oriented nanocrystals. The copolymer chosen for this study has a 90% volume fraction of PS and 10% volume fraction of P4VP. Such low fractions of P4VP or P4VP+HABA ensure the formation of spherical/cylindrical domains parallel or perpendicular to the surface, embedded in the PS matrix. The pyridine group of P4VP interacts with HABA; this latest molecule forms a hydrogen bonding complex with the P4VP via its carboxyl group. The copolymer + HABA film dip-coated onto the silicon surface has an average thickness of 45nm, corresponding to the solution concentration of 1,5%. This PS-P4VP +HABA phase separation is enhanced by a solvent annealing that mainly produces a high degree of long-range lateral order of cylindrical domains oriented normal or perpendicular to the surface. This solvent treatment represents a driving force to order phase-separated block copolymer films in lateral dimensions. After this phase separation step and HABA removal, the surface morphology was visuliazed by AFM. Typical AFM pictures demonstrating the surface morphology of PS-P4VP thin film of different thickness are given in Figure 2.

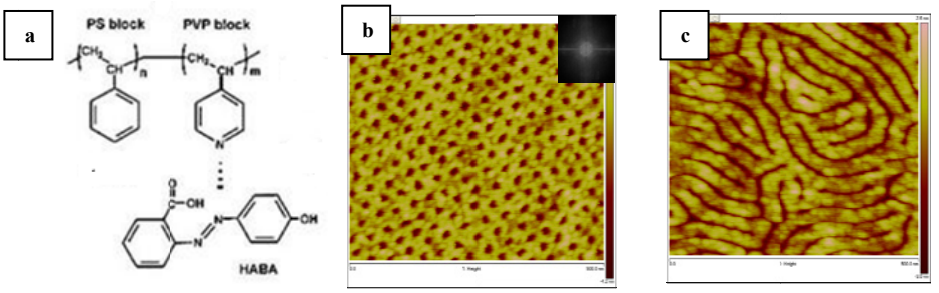

Figure 2: A. Scheme depicting the hydrogen interaction between diblock PS-P4VP copolymer and HABA, B .Height AFM image of long-range hexagonal order of cylindrical domains oriented normal to the surface, frame size: 500nm. The inset is the FFT plot of the image C. lamellar structure of diblock copolymer , frame size: 500nm

The AFM image of the copolymer matrix coated on solvent cleaned silicon surface (Figure 2B) shows, after removal of the HABA, a hexagonal arrangement of the cylindrical nanoholes. The film thickness is of ~ 42.5 nm. Figure 2A shows a center-to-center distance *d* between two nanopores of 20 ± 3.0 nm.

The AFM image in Figure 3C shows ordered domains that exhibit mainly hexagonal packing with some square oriented lattices. Such unusual square packing was also observed in the case of triblock copolymer[24]. Previous reports have explained the strong influence of the film thickness on the packing of the structure and the possibility of coexistence of two different structures in the same film. In addition,

it has also been shown that the ordering behavior of block copolymer during solvent annealing was highly dependent on the amount of residual salt remaining in the copolymer [25] from the initiator during synthesis. Hence, the lower the film thickness is, the more the long-range lateral order of cylindrical domains oriented parallel to the surface is, as displayed in Figure 2C.
After argon treatment to remove the PVP residual thin film at the bottom of the nanoholes, the copolymer film thickness decreased from an average of 42.5 down to 29 nm.
Finally, the formation of a complex between P4VP residual chains inside the nanoholes and Au cations has been favored by the addition of metal salt in the system. An acid-base interaction between tetrachloroauric acid and pyridine group or an electrostatic interaction between pyridinium salts formed by the protonation of pyridine and gold ion is indeed possible as it was reported previously[26].

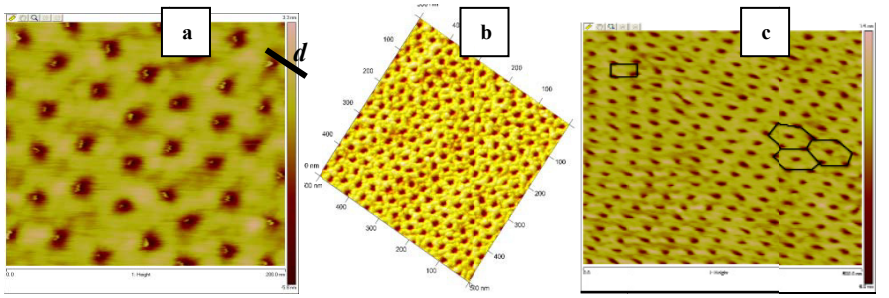

Figure 3: A. Height AFM image of an Array of nanoholes in thin copolymer film PS-P4VP copolymer , frame size: 200nm; B 3D Height AFM image of PS-P4VP copolymer film , frame size: 500nm. C. Height AFM image of PS-P4VP copolymer film presenting both hexagonal and square packing, frame size: 500nm

Au nanoparticles were prepared by reduction of gold salt in the presence of Hydrazine or NaBH4. After dissolving $HAuCl_4$, the solution is rapidly stirred while a reducing agent is added. This causes Au^{3+} ions to be reduced to neutral gold atoms. As more and more of these gold atoms form, gold gradually starts to precipitate in the form of sub-nanometer particles. The rest of the gold atoms that form sticks to the existing particles with a rather uniform size [27]. After exposing the sample to oxygen plasma, the polymer matrix is removed from the surface. It can be seen that the gold nanoparticles (12 nm diameter) formed, were confined within the preformed nanoholes as displayed in Figure 3. Additionally, the average nanoparticle surface coverage is of the order of 70% of the surface.

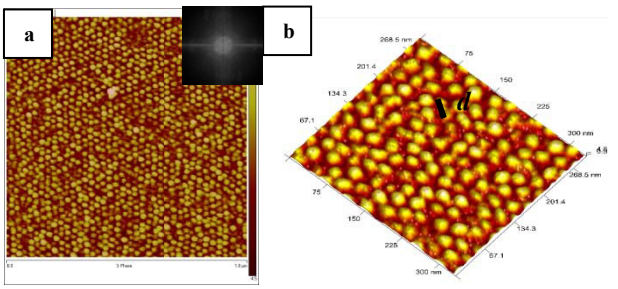

Figure 4: A. Height AFM image of an array of gold nanoparticles assembled on a silicon surface , frame size: 1µm; The inset is the FFT plot of the image B. 3D Height AFM image of an array of gold nanoparticles assembled on a silicon surface frame size: 300nm.

The center-to-center average distance between Au particle is approximately 20 nm spacing as displayed in Figure 4B. The average gold nanoparticle diameters according to AFM height estimations were 12 nm. Assuming a Gaussian distribution of nanoparticle size, the standard deviation is less than 10%, indicating

that this block copolymer template method is a very effective means to generate uniformly sized gold nanoparticles. The 2D nanoparticle coverage on the substrate represents the order of 70% of the total surface. This alternative process combining self-assembly and soft synthesis route has enabled to create highly ordered and uniformly sized nanoparticles. In addition, XPS measurements have proved the presence of pure metallic Au(0).

In Figure 5, Au $4f_{7/2}$ appears at 83.5 eV, indicating that Au is in the form of Au(0). Typically, the peak from Au_2O_3 is around 85.9 eV [28]. This result can be explained by the facile reduction of an oxidized gold species to its zero-valent state. The most stable state for gold is the zero-valent state. Although Au(+3) was used as the gold precursor and plasma treatment was used in the process to remove all of the organic components and only Au(0) was detected.

Finally, the use of block copolymers that self-assemble to form periodic structures with well-defined size and periodicity on a scale of tens of nanometers represent an easy way to assemble nano-objects. Variation of the molecular weight of the copolymer should enable a control over the size and periodicity of the cylindrical nanopores and therefore of the resulting metallic structures. Although we demonstrate only the formation of gold nanostructures, this method may be applied to the deposition of many other metals available for soft synthesis route[29]. For these reasons, this route to the generation of arrays of nanostructures is particularly attractive in terms of simplicity and flexibility.

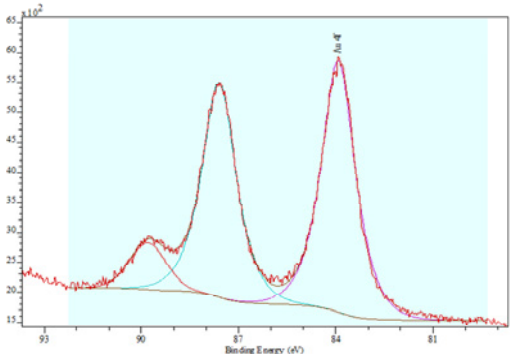

Figure 5: Experimental XPS spectrum performed on a hexagonal array of Au nanoparticle.

4. Conclusion

In summary, very simple routes to generate nanoscopic arrays of metal nanoparticles are presented. First, we have reported block-copolymer (BCP) thin films self-assembled in a well-defined hexagonal morphology. This process expands to the use of polymer films having cylindrical domains, which have the advantage of being used both as negative and positive templates. Filling the organic porous mask by a salt that constitutes the precursor for the nanoparticle for the colloidal synthesis via a soft, aqueous liquid-based route, offers quite a few advantages. We have shown that polymer-metal salt complexation combined with chemical reduction affords a simple, yet robust, route to control the size and lateral ordering of nanopartcile in thin films of block copolymer. This strategy is general and can be extended to any block copolymer where one of the components can form a complex with a heavy metal ion salt. Therefore, this general strategy allows one to generate functional, self-orienting, self-assembling systems that hold promise in the fabrication of nanostructured materials where the spatial placement of each element can be controlled and, as such, opens a pathway to addressable media.

Acknowledgment. We are grateful to the support by the CNRS, Université de Haute Alsace for the financial support as well as the Lebanese University in Beirut.

References

[1] C.Park, J.Yoon, E. L. Thomas, Polymer 44 (2003) 6725.
[2] J. Y. Cheng, C. A. Ross, H. I. Smith, E. L. Thomas, Adv. Mater. 18 (2006) 2505.
[3] T. L. Sounart, J. Liu, J. A. Voigt,J. W. P. Hsu, E. D. Spoerke, Z. R.. Tian, Y. Jiang, Adv. Funct. Mater. 16 (2006) 335.
[4] M. A. McCord, M. J. Rooks, Handbook of Microlithography, Micromachining,and Microfabrication, Vol. 1 (Ed: P. R. Choudhury), SPIE, Bellingham,WA 1997
[5] X. Liu, M. Stamm, Nanoscale Res Lett. 4. (2009) 459.
[6] Turner APT. Biosensors: Past, present and future; 1996. http://www.cranfield.ac.uk/biotech/chinap.htm.
[7] H-W. Li, W. T. S. Huck, Nano Letters 4 (2004) 1633.
[8] I.W. Hamley, Progress in Polymer Science 34(2009) 1161.
[9] M. A. Hillmyer, Adv Polym Sci. 190 (2005) 137.
[10] S. Krishnamoorthy, C. Hinderling, H. Heinzelmann, Materials Today 9 (2006) 40.
[11] E. D. Spoerke, M. T. Lloyd, Y.-J. Lee, T. N. Lambert, B. B. McKenzie, Y-B. Jiang, D. C. Olson, T. L. Sounart,J. W. P. Hsu, J. A. Voigt J. Phys. Chem. C 113(2009) 16329.
[12] W. I. Park, G.-C. Yi, M. Kim, S. J. Pennycook, Adv. Mater. 14(2002) 1841.
[13] L. C. Chen, S. W. Chang, C. S. Chang, C. Y. Wen, J.-J. Wu, Y. F. Chen, Y. S. Huang, K. H. Chen, J. Phys. Chem. Solids 62 (2001) 1567.
[14] Z. F. Ren, Z. P. Huang, J. W. Xu, J. H. Wang, P. Bush, M. P. Siegel, P. N. Provencio, Science 282 (1998) 1105.
[15] O. Seifarth , R. Krenek, I. Tokarev , Y. Burkov, A. Sidorenko, S. Minko,M. Stamm, D. Schmeiβer, Thin Solid Films 515 (2007) 6552.
[16] H. Yu, Z. Zhang, M. Han, X. Hao, F. Zhu, J. Am. Chem. Soc. 127 (2005) 2378.
[17] X. Gao, Z. Zheng, H. Zhu, G. Pan, J. Bao, F. Wu, D. Song, Chem.Commun. (2004) 1428.
[18] R. Liu, F. Oba, E. W. Bohannan, F. Ernst, J. A. Switzer, Chem. Mater. 15 (2003) 4882.
[19] T. H. Kim, J. Huh, J. Hwang, H-C. Kim, S. H. Kim, B-H. Sohn, C. Park, Macromolecules 42(2009) 6688.
[20] H. G. Boyen, G. Kastle, F.Weigl, B. Koslowski, C. Dietrich, P. Ziemann, J. P. Spatz, S. Riethmuller, C. Hartmann, M. Moller, G. Schmid, M. G. Garnier, P. Oelhafen, Science 297 (2002) 1533.
[21] J. P. Spatz, S. Mossmer, C. Hartmann, M. Moller, T. Herzog, M. Krieger, H. G. Boyen, P. Ziemann, B. Kabius, Langmuir 16 (2000) 407.
[22] Jaramillo, T. F.; Baeck, S. H.; Roldan Cuenya, B.; McFarland, E. W. J.Am. Chem. Soc. 125 (2003) 7148.
[23] R. M. A. Azzam, N. M. Bashara, Ellipsometry and polarized light; North-Holland Pub. Co.: Amsterdam ; New York New York, 1977.
[24] C. Tang, J. Bang, G. E. Stein, G. H. Fredrickson,C. J. Hawker, E. J. Kramer, M. Sprung, J. Wang Macromolecules 41(2008) 4328.
[25] S. H. Kim, M. J. Misner, T. Xu, M. Kimura, T. P. Russell, Adv.Mater. 16 (2004)226.
[26] C-P. Li, C-H. Wu, K-H. Wei, J-T. Sheu, J. Y. Huang, U-S. Jeng, K. S. Liang Adv. Funct. Mater. 17(2007) 2283.
[27] T. Lohmueller, E. Bock, J. P. Spatz Adv. Mater. 20(2008) 2297.
[28] C. D. Wagner, W. M. Riggs, L. E. Davis, J. F. Moulder, Handbook of X-ray Photoelectron Spectroscopy, 1st ed., Perkin Elmer Corporation, Eden Prairie, MN 1979.
[29] H. Yang, H. Zeng, J. Am. Chem. Soc. 127 (2005) 270.